SUPPLEMENTAL MATERIAL

Miyauchi et al., http://www.jem.org/cgi/content/full/jem.20091957/DC1

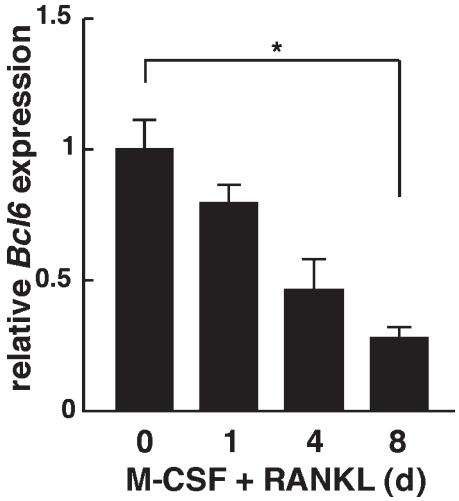

Figure S1. Bcl6 expression is suppressed during osteoclastogenesis induced by RANKL. BMMs were treated with 25 ng/ml RANKL for indicated periods, and *Bcl6* expression relative to *β-actin* was analyzed by quantitative real-time PCR analysis. Data are means ± SD of *Bcl6*/*β-actin* of RANKL-treated cells compared with nontreated cells (*, $P < 0.01$; $n = 5$). Representatives of at least three independent experiments are shown.

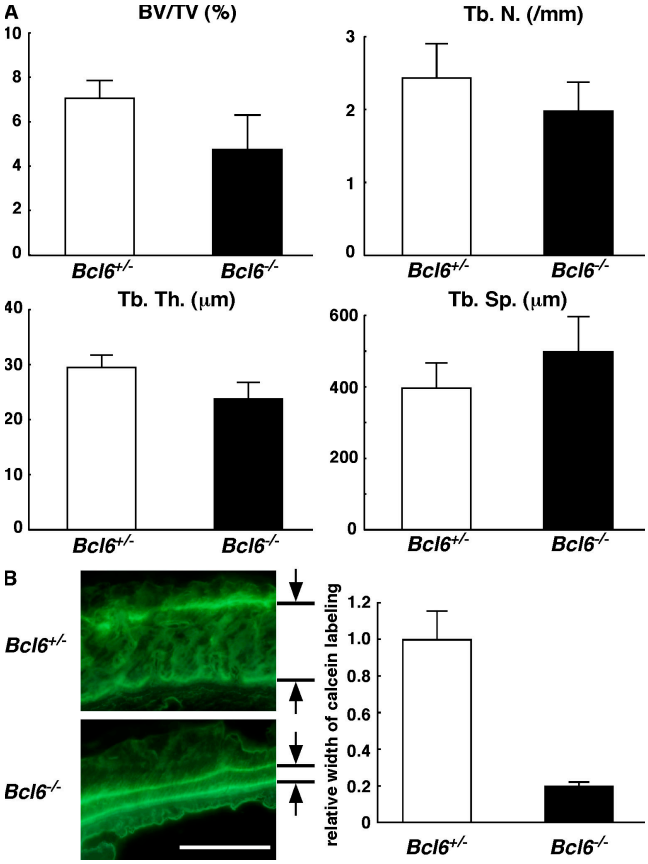

Figure S2. Bone parameters of Bcl6$^{-/-}$ mice. (A) Results of bone histomorphometric analysis. Data are mean bone volume per total volume (BV/TV; %), trabecular number (Tb. N; /mm), trabecular thickness (Tb. N; μm), or trabecular separation (Tb. Sp; μm) ± SD of *Bcl6*$^{+/-}$ (white bars) and *Bcl6*$^{-/-}$ (shaded bars) mice (n = 5). (B) Calcein was injected 6 and 1 d before analysis, and calcein labeling was observed under a fluorescence microscope. (left) Representative data. (right) Data are mean ± SD of calcein labeling in *Bcl6*$^{+/-}$ (white bar) and *Bcl6*$^{-/-}$ (shaded bar) mice (n = 5).

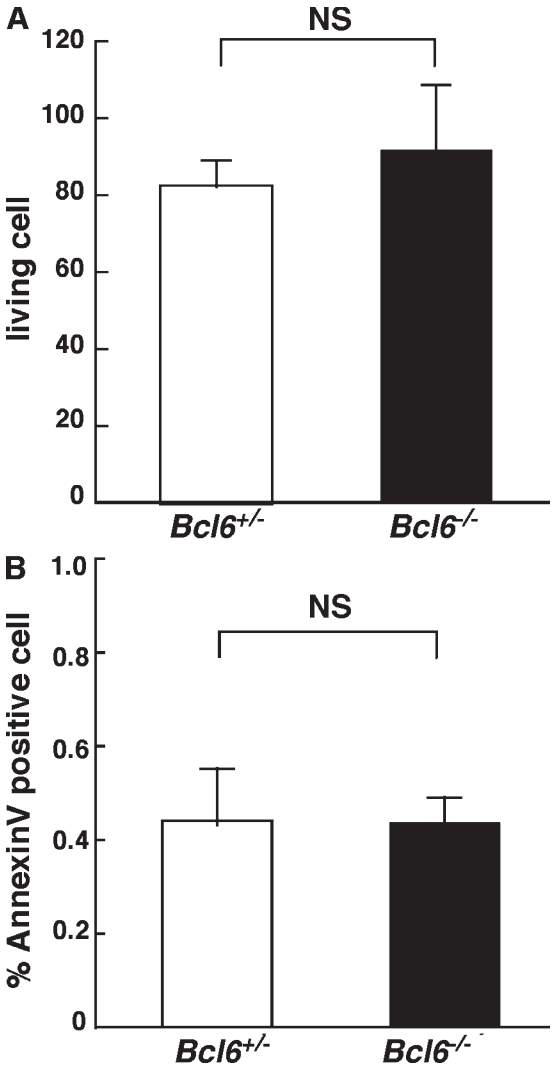

Figure S3. Proliferation and apoptosis of *Bcl6*$^{-/-}$ osteoclast precursors. M-CSF–dependent osteoclast precursors were isolated from *Bcl6*$^{+/-}$ (white bars) and *Bcl6*$^{-/-}$ (shaded bars) mice and subjected to proliferation and apoptosis assays. (A) Osteoclast precursors were cultured with M-CSF for 3 d, stained with trypan blue, and cell number was determined. Data are shown as mean number of live *Bcl6*$^{+/-}$ (white bar) and *Bcl6*$^{-/-}$ (shaded bar) cells ± SD. (B) *Bcl6*$^{+/-}$ (white bar) and *Bcl6*$^{-/-}$ (shaded bar) osteoclast progenitors were stained with FITC-conjugated Annexin V, and the proportion of apoptotic cells was analyzed by FACSCalibur. Data are shown as mean proportion of apoptotic cells in *Bcl6*$^{+/-}$ (white bar) and *Bcl6*$^{-/-}$ (shaded bar) cells ± SD. Three representative, independent experiments are shown.

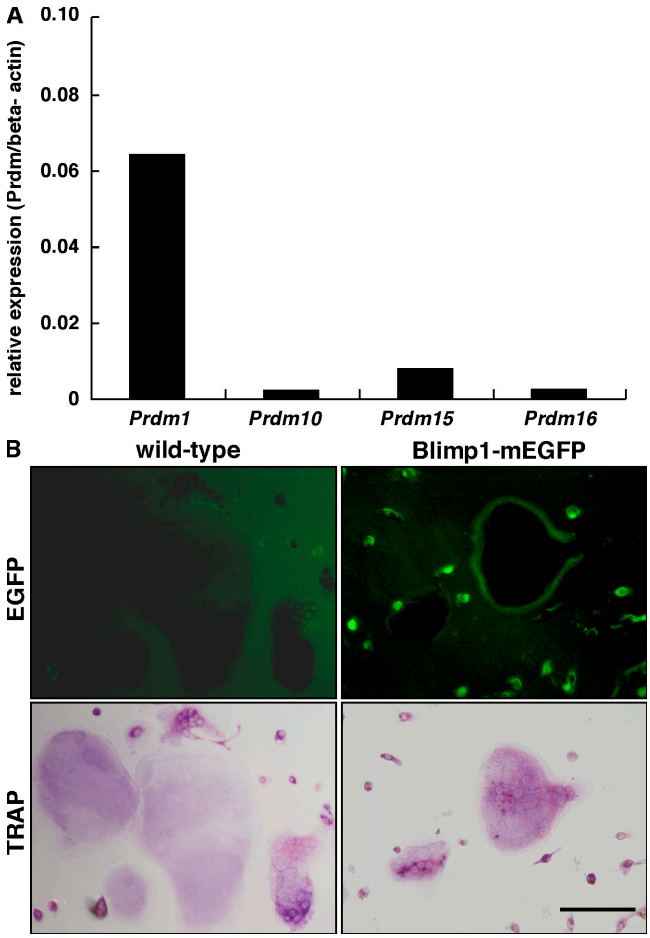

Figure S4. Blimp1 is expressed in osteoclasts. (A) Comparative expression analysis of *Prdm* family genes. BMMs were cultured with RANKL and subjected to GeneChip analysis. (B) BMMs were prepared from wild-type and Blimp1-mEGFP BAC transgenic mice, and osteoclast differentiation was induced by RANKL stimulation. Blimp1 expression and osteoclast differentiation were analyzed by mEGFP expression using fluorescence microscopy (top) and TRAP staining (bottom), respectively. Representatives of at least three independent experiments are shown.

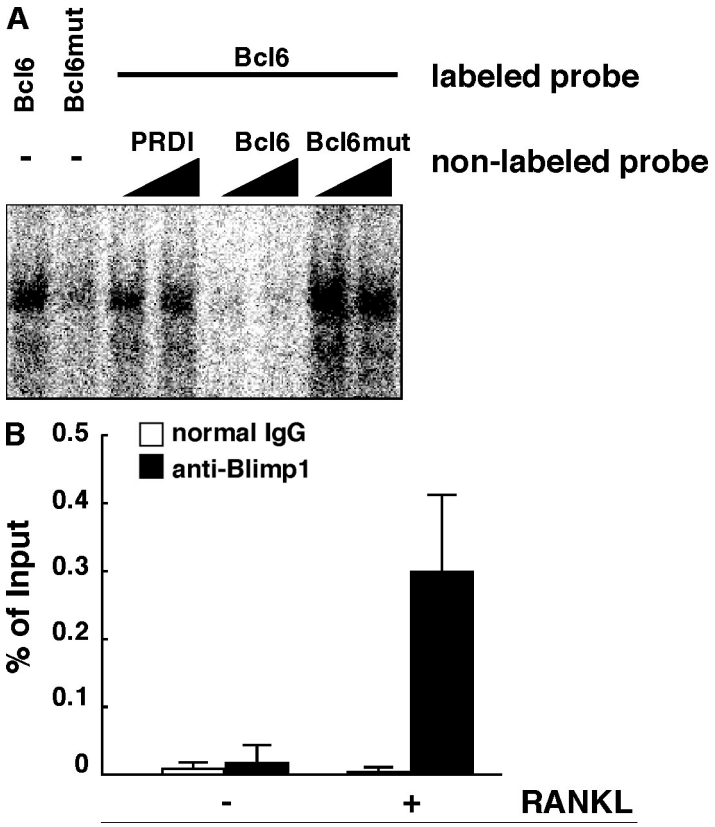

Figure S5. Blimp1 binds sequences in the Bcl6 promoter. (A) Nuclear extracts were prepared from Blimp1-transfected COS7 cells. Complexes of Blimp1 and labeled probes containing Bcl6 or mutated Bcl6 (Bcl6mut) binding site were analyzed in the presence or absence of indicated unlabeled probes by EMSA. (B) M-CFS–dependent osteoclast progenitor cells were stimulated by M-CSF and RANKL for 4 d. Nuclear extracts were then isolated and ChIP undertaken using an anti–Blimp1 antibody. ChIP fractions were analyzed by real-time PCR with primers specific for the *Bcl6* promoter. Results are shown as mean intensity relative to input percentage ± SD. Three representative, independent experiments are shown.

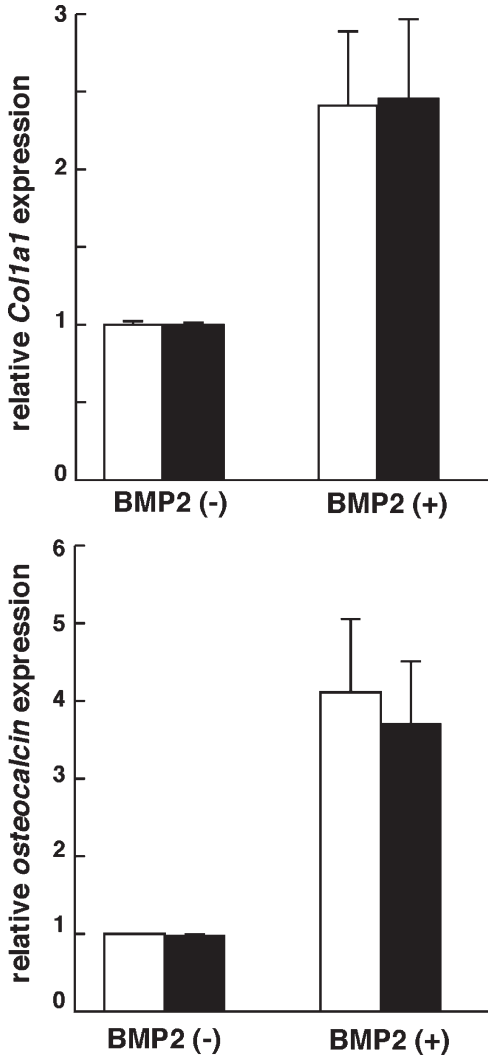

Figure S6. Primary osteoblasts from control or Blimp1 cKO mice express bone matrix genes. Primary osteoblasts isolated from calvaria of control (white bars) or Blimp1 cKO (shaded bars) mice were cultured in the presence or absence of BMP2 for 4 d. Expression of *type I collagen* (*Col1a1*) and *osteocalcin* was analyzed by realtime PCR and normalized to *β-actin*. Data are shown as mean ± SD of *Col1a1* or *osteocalcin* relative to *β-actin*. Four representative, independent experiments are shown.

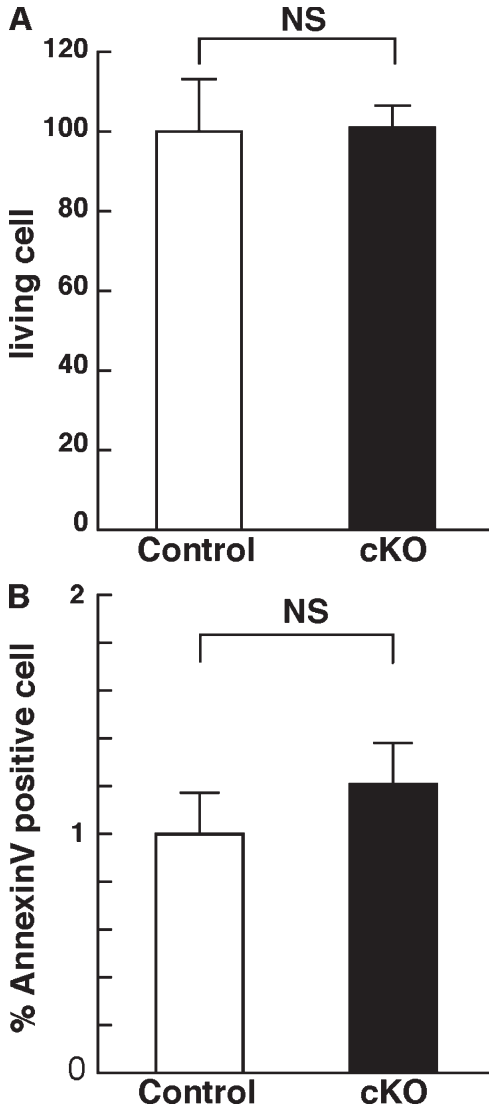

Figure S7. Proliferation and apoptosis of osteoclast precursors in Blimp1 cKO mice. M-CSF–dependent osteoclast precursors were isolated from control (white bars) and Blimp1 cKO (shaded bars) mice and subjected to proliferation and apoptosis assays. (A) Osteoclast precursors were cultured with M-CSF for 3 d, stained with trypan blue, and cell number was determined. Data are shown as mean live cells in control (white bar) and Blimp1 cKO (shaded bar) cells ± SD. (B) Control (white bar) and Blimp1 cKO (shaded bar) osteoclast progenitors were stained with FITC-conjugated Annexin V, and the proportion of apoptotic cells was analyzed by FACSCalibur. Data are shown as mean proportion of apoptotic control (white bar) and Blimp1 cKO (shaded bar) cells ± SD. Three representative, independent experiments are shown.

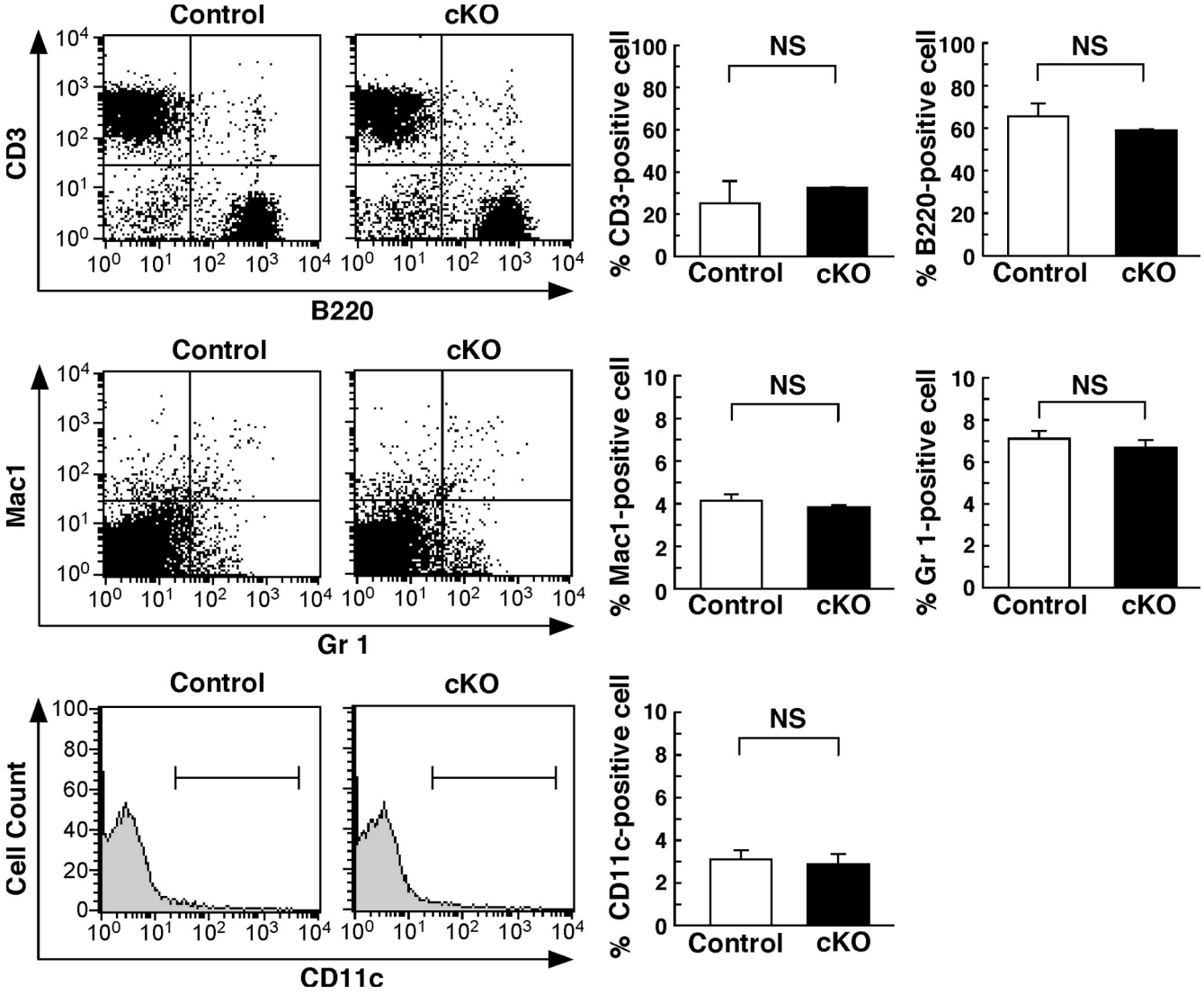

Figure S8. Immune cell populations in Blimp1 cKO mice. Mononuclear splenocytes were isolated from Blimp1 cKO and control mice, stained with anti–CD3-PE (500A2) + anti–B220-FITC (RA3-6B2), anti–Gr1-FITC (RB6-8C5) + anti–Mac1-PE (M1/70), or anti–CD11c-PE (HL3), and subjected to FACS analyses. Results are shown as mean percentage ± SD.

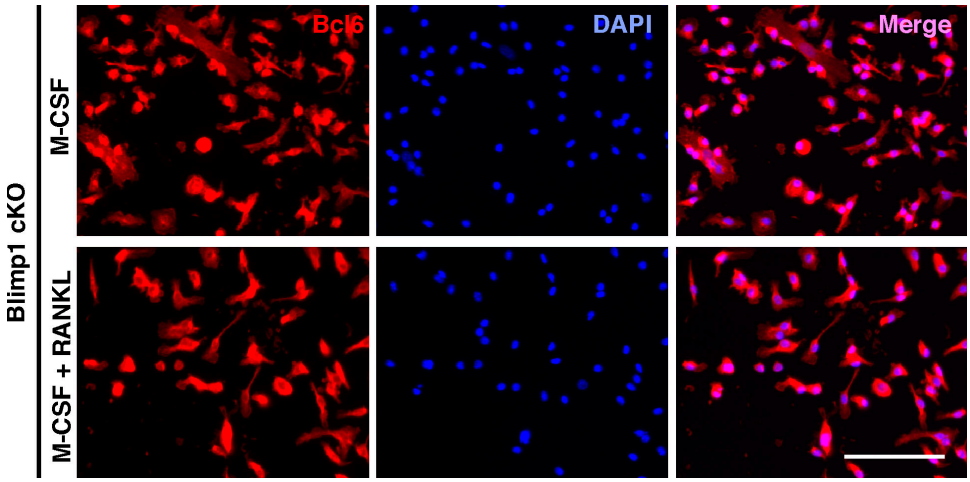

Figure S9. Dysregulation of Bcl6 in Blimp1 cKO BMMs after RANKL treatment. Blimp1 cKO or control BMMs were cultured in the presence of M-CSF alone or M-CSF plus RANKL for 6 d and subjected to immunofluorescent staining for Bcl6. DAPI was used as nuclear staining. Bcl6 expression was maintained in Blimp1 cKO cells even in the presence of RANKL. Representatives of at least two independent experiments are shown.